

# Short visit to Würzburg: Using different PTCDI molecules as n-type organic materials in diode configuration

David Cheyns

Period: 10/04/2007 till 20/04/2007

*People involved: Andreas Baumann, Matthias Roos, Carsten Deibel (Würzburg), Claudio Girotto, David Cheyns, Jan Genoe (imec)*

## 1 Purpose of the visit

Efficient organic solar cells consist of at least two materials, namely a donor material and an acceptor material. The most widely used family of acceptor materials are the fullerenes. In polymer blends, PCBM<sup>1</sup> is used as most efficient acceptor, while in small molecule solar cells C<sub>60</sub> beats everything. Another class under investigation are the perylene-derivatives. High n-type transistor mobilities have been demonstrated for polycrystalline films based on perylene diimides [1, 2, 3]. These materials have a large electron affinity and they assemble in  $\pi$ -stacks which enhances intermolecular  $\pi$ -orbital overlap, improving charge transport.

During this visit, three commercial available perylene derivatives are studied for the use in solar cells, namely *N,N'*-Dialkyl-3,4,9,10-perylene tetracarboxylic diimides with alkyl=pentyl (PTCDI-C5), tridecyl (PTCDI-C13), and phenyl (PTCDI-Ph). Important factors for a good acceptor material are (1) the vertical transport properties, (2) the absorption in the solar cell spectrum and (3) the morphology. The vertical transport properties are studied using photo-CELIV (Carrier Extraction by a Linearly Increasing Voltage) (done at Würzburg). Absorption spectra are measured using Ultraviolet-visible spectroscopy (Würzburg) and ellipsometry (imec). The last factor, the morphology, is studied with Scanning Electron Microscopy (imec) and Atomic Force Microscopy (imec).

We conclude that PTCDI-C13 and PTCDI-Ph are two interesting materials, where PTCDI-C13 has a higher mobility and PTCDI-Ph shows a higher absorption and a better morphology.

## 2 Experiments

The organic materials *N,N'*-Dialkyl-3,4,9,10-perylene tetracarboxylic diimide with alkyl=pentyl (PTCDI-C5), tridecyl (PTCDI-C13), and phenyl (PTCDI-Ph)(figure 1), are used as purchased (Aldrich) with a purity of  $\geq 98\%$ . After loading in high vacuum, a dummy run is done to remove possible contaminations. In this run, the material is evaporated at a slightly higher temperature compared to the temperature that will be used in subsequent evaporations. Samples (both glass, glass/ITO and silicon) are cleaned before the evaporation. In a first stage, the samples are cleaned with solvents (acetone and IPA, 10 minutes ultrasonic each). Subsequent, the samples undergo 10 minutes treatment with oxygen plasma.

The evaporations are done in high vacuum ( $10^{-6}$  torr) with a flux around  $1 \text{ \AA}/\text{s}$ . The conditions are kept the same for all the used molecules. For the diodes, 80nm aluminum is evaporated on top

---

<sup>1</sup>[6,6]-phenyl-C61 butyric acid methyl ester

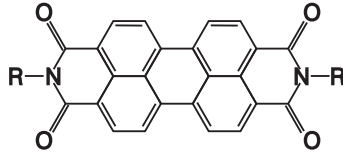


Figure 1: Molecular structure of *N,N'*-Dialkyl-3,4,9,10-perylene tetracarboxylic diimide. The alkyl-sidechain R corresponds to pentyl (PTCDI-C5), tridecyl (PTCDI-C13), and phenyl (PTCDI-Ph)

of the organic to create a sandwiched structure ITO/organic/Aluminum with a size of  $3\text{mm}^2$ . The aluminum evaporation is carried out in the same high vacuum chamber, after adding a shadowmask (change of shadowmask takes place in air). The samples are transferred to a nitrogen glovebox, using a closed container filled with argon.

## 2.1 Vertical transport properties

The two most widely used methods to experimentally determine the mobility of carriers in organic layers, are not suitable when working with thin film (below  $1\mu\text{m}$ ) diode structures. The first method calculates the mobility from the transfer characteristics of field effect transistors. Carriers in the transistor structure follow the surface of an insulating dielectricum. This surface has a huge impact on the mobility of the carriers[4, 5]. As a result, this method is not representable for the carrier flow in a diode structure. The second method uses a time-of-flight (TOF) method. The necessity to have a high optical density for the used films, create a constraint on the thickness that can be used (at least  $1\mu\text{m}$  for high absorbing organic materials)[6].

A solution to calculate mobilities in thin film organic diodes, was presented by Juška et al[7, 8]. The method is called Carrier Extraction by Linearly Increasing Voltage (CELIV) and is based on equilibrium charge extraction. As demonstrated in figure 2, two consecutive pulses of linearly increasing voltage are applied to a diode with at least one blocking contact, and the current transients related to extraction of equilibrium carriers are monitored. Extracted charge is equal to the difference of these two transients for sufficiently small delay ( $t_d$ ). Increase of this delay allows the monitoring of the recovery of equilibrium. The second pulse can be used to determine noideal conditions like non-perfectly blocking contacts. From the current characteristics, the capacity and the mobility of the layer can be calculated (for a detailed mathematical study, see Juška et al[7, 8]).

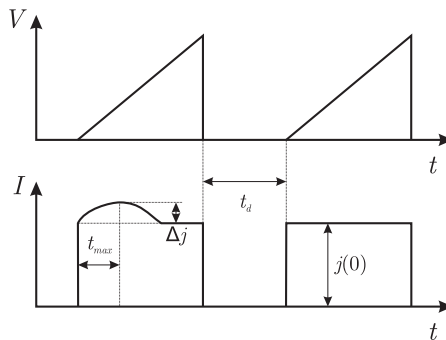


Figure 2: Schematic illustration of the CELIV method

A short light pulse can be used to increase the number of extracted carriers (photo-CELIV[9, 10]). In this case, the light pulse is applied before the first linearly increasing voltage ramp. This light pulse creates excitons, which will be dissociated at traps, creating free or trapped carriers. The delay in between the pulse and the ramping voltage should be smaller than the relaxation of the created carriers and big enough to not see any displacement currents introduced by the light

pulse.

From the initial step, the combination of thickness ( $d$ ) and permittivity  $\epsilon\epsilon_0$  can be calculated:

$$j(0) = \epsilon\epsilon_0 A/d \quad (1)$$

with  $A$  the slope of the linearly increasing voltage ( $V(t) = At$ ). The mobility can be estimated taking into account some numerical estimations[8]:

$$\mu = \frac{2d^2}{3At_{max}^2 \left[ 1 + 0.36 \frac{\Delta j}{j(0)} \right]} \quad (2)$$

The results for PTCDI-C5 can be seen in figure 3. By playing with ramping speed  $A$ , the field dependence of the mobility can be measured (figure 3(a)). The field is calculated using the voltage applied at the point of  $t_{max}$ , assuming a uniform field distribution, and corrected for the build-in voltage. As the samples are mounted in a cryostat, the second parameter that can be changed is the temperature. When the temperature is lowered, the mobility will go down. The decreasing mobility corresponds to a shift of  $t_{max}$  to larger delays, and as a result higher voltages and higher fields are typically encountered.

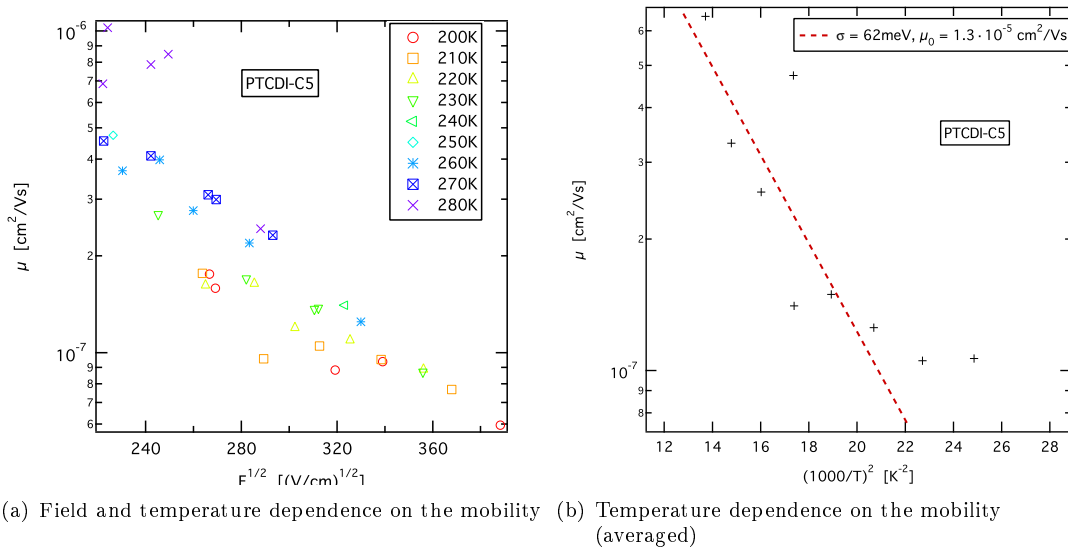


Figure 3: Results of the photo-CELIV measurement for PTCDI-C5

Figure 3(b) plots the mean value of the field-dependent mobility versus temperature. This holds as long as the scatter from the field-dependency is low. The scatter for PTCDI-C5 is actually high (almost an order of magnitude for 280K), so the resulting temperature dependent plot should be taken with care. The disorder formalism developed by Bäessler and coworkers[11] is used to analyze the temperature dependence of the mobility. The formula used is:

$$\mu(T) = \mu_0 \exp \left[ -\frac{2}{3} \left( \frac{\sigma}{kT} \right)^2 \right] \quad (3)$$

where  $\mu_0$  is a prefactor mobility in the energetically disorder-free system and  $\sigma$  is the width of the assumed Gaussian distribution of states. The resulting values for PTCDI are  $\mu_0 = 1.3 \times 10^{-5} \text{ cm}^2/\text{Vs}$  and  $\sigma = 62 \text{ meV}$ . A second trap distribution can be seen at lower temperatures, but due to the high scatter and the few points, no attempts are made to fit this data.

The second material measured with photo-CELIV is PTCDI-C13 (figure 4). This derivative shows the highest transistor mobilities in literature[3], due to the longer side-chains, aiding self-assembly. The results of CELIV measurements presented here show a high mobility (in the range

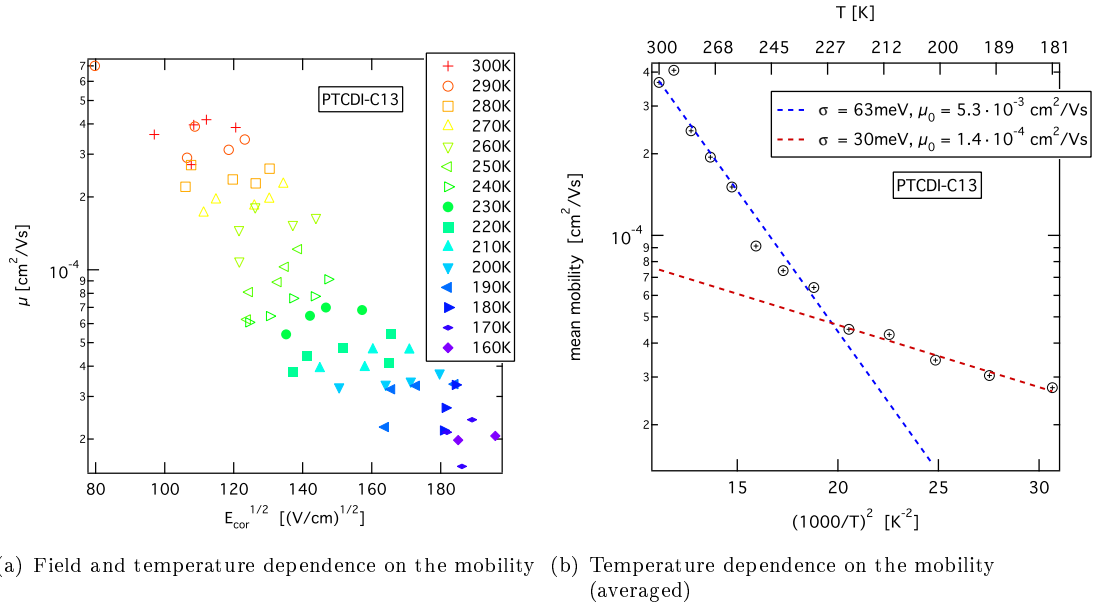


Figure 4: Results of the photo-CELIV measurement for PTCDI-C13

of  $10^{-4} \text{cm}^2/\text{Vs}$ ) and a low field dependency. As this dependency is low, the used technique to take the mean-mobility at each temperature is trustworthy. Using equation 3, two different trap distribution can be seen. Shallow traps with a Gaussian distribution of states width  $\sigma = 30 \text{meV}$  and  $\mu_0 = 1.4 \times 10^{-4} \text{cm}^2/\text{Vs}$ , are only visible at low temperatures. The deeper traps are activated at higher temperatures, and corresponds to  $\sigma = 63 \text{meV}$  and  $\mu_0 = 5.3 \times 10^{-3} \text{cm}^2/\text{Vs}$ .

The results of the photo-CELIV measurements on PTCDI-Ph can be seen in figure 5. This material was used in on of the first efficient n-type transistors based on perylene[1]. The mobility calculated by CELIV is in the range of  $10^{-5} \text{cm}^2/\text{Vs}$ , which is one order of magnitude lower than the mobility of PTCDI-C13.

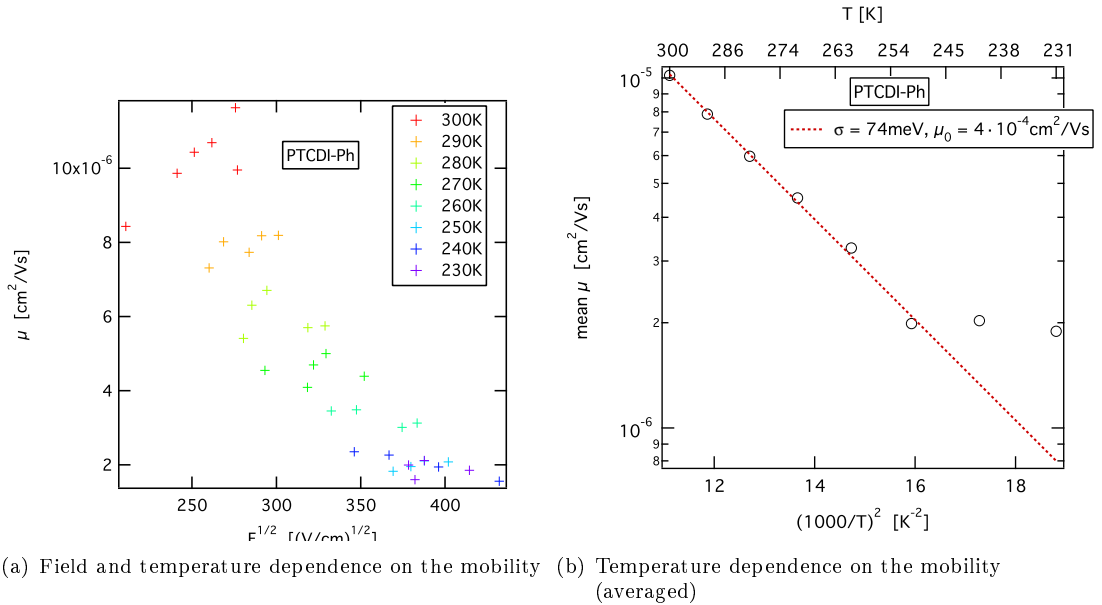


Figure 5: Results of the photo-CELIV measurement for PTCDI-Ph

Again, due to the low field-dependency, the temperature plot 5(b) is trustworthy. A second trap density can be seen at low temperatures, but too few points are measured for a reliable fit. The results at high temperatures give  $\sigma = 74meV$  and  $\mu_0 = 4 \times 10^{-4}cm^2/Vs$ .

## 2.2 Absorption profile

Absorption spectra are measured using Ultraviolet-visible spectroscopy (UV-VIS) and ellipsometry. Thin films of organic material are deposited on transparent glass substrates. These samples are used for UV-VIS measurement and the result can be seen in figure 6.

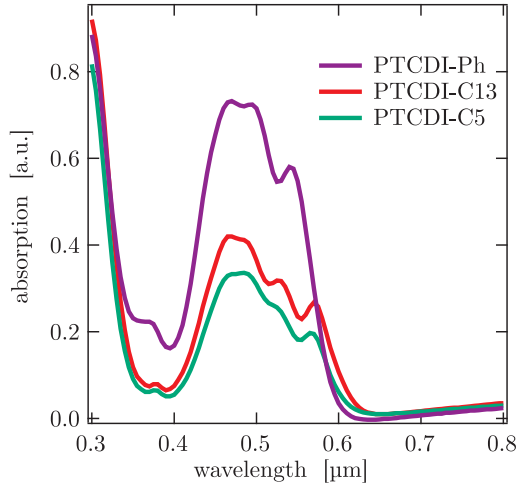


Figure 6: Absorbance of the different PTCDI films

Transferring absorbance data to absorption coefficient can be done assuming an exponential decay of light in the film, which is not necessarily true for thin layers as optical interference can occur. Nevertheless, by combining the data from figure 6 and thickness measurements from SEM (see section 2.3) some first conclusions can be drawn. The measured thickness for PTCDI-C5, PTCDI-C13 and PTCDI-Ph is 64nm, 200nm and 160nm resp. As PTCDI-C13 and PTCDI-Ph are in the same thickness-range, the absorbance data can be compared directly. Due to the higher absorbance of PTCDI-Ph, this molecule will probably have a higher absorption coefficient compared to PTCDI-C13. The layer of PTCDI-C5 is three times as thin compared to PTCDI-C13, while the absorbance data are comparable. Also in this case, PTCDI-C5 will have a higher absorption coefficient.

Organic layers deposited on Si/SiO<sub>2</sub> are used to determine the complex index of refraction with ellipsometry (SOPRA, ges5). The resulting values can be seen in figure 7. The fitting of the PTCDI-C5 failed as the resolution of the obtained data was not high enough (probably due to the thinner layer). The assumption made from the absorbance data are confirmed looking at the values of the extinction coefficient  $k$ . This coefficient is related to the absorption coefficient  $\alpha$  by the formula  $\alpha = 4\pi k/\lambda$ , with  $\lambda$  the wavelength used. As the extinction coefficient of PTCDI-Ph is twofold higher than the extinction coefficient of PTCDI-C13, a twofold increase in absorption is expected for the same layer thickness. Another parameter calculated during fitting of ellipsometry data, is the thickness of the layers. The values are 210nm for PTCDI-C13 and 170nm for PTCDI-Ph, which corresponds closely to the thickness determined by SEM (section 2.3).

## 2.3 Morphology

The study of the morphology is carried out using a Scanning Electron Microscope (Philips, XL30) and an Atomic Force Microscope (Molecular Imaging, PicoLE). The morphology of PTCDI-C5 can be seen in figures 8 and 9. The layer is very smooth (root-mean-square (rms) value of 2nm) and a

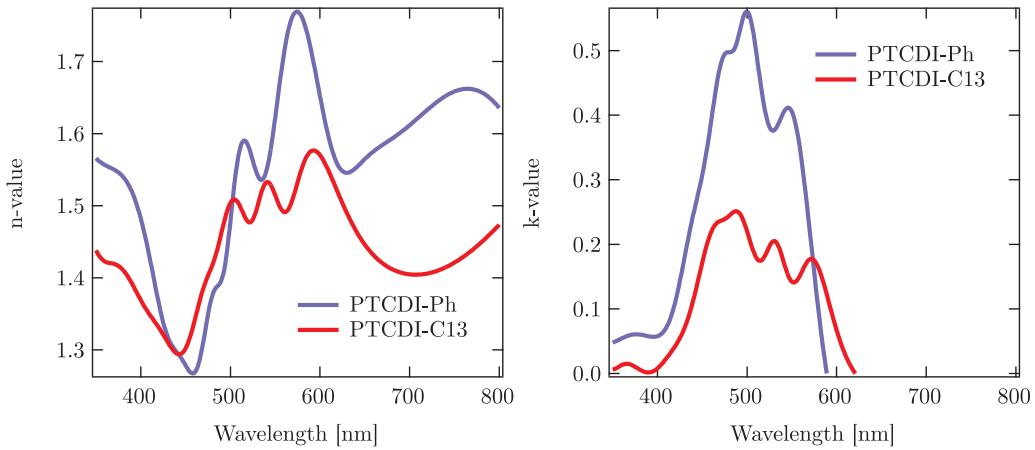


Figure 7: Complex index of refraction  $n + ik$ , fitted using ellipsometry data. Left: refractive index  $n$ , right: extinction coefficient  $k$

thickness of 65nm can be determined by cross-section SEM. AFM visualizes Small grains (400nm by 100nm) with molecular terraces around 1.6nm inside the grain. These terraces correspond to the d-spacing in between two layers, as confirmed by XRD[2].

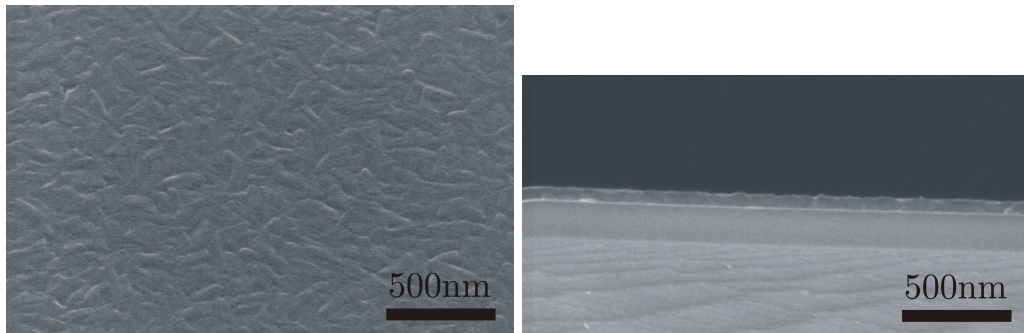


Figure 8: SEM picture of PTCDI-C5, top view (left) and crosssection view (right)

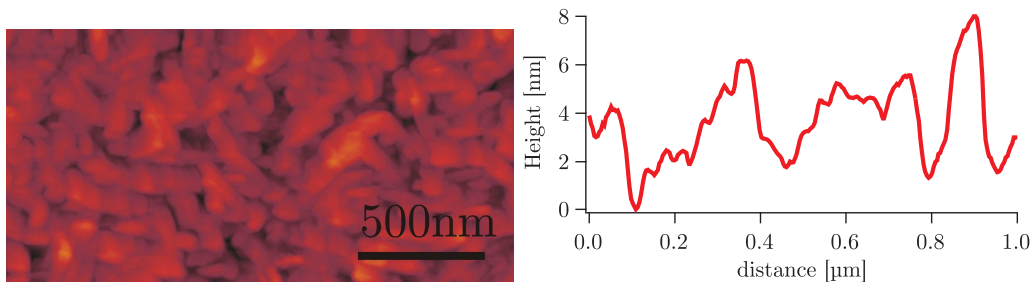


Figure 9: AFM picture of PTCDI-C5, top view (left) and a crosssection (right)

The layer of PTCDI-C13 is much rougher (rms value of 43nm) and needles or disks can be found on top of a more smooth layer. The thickness of the smooth layer is around 200nm, while the needles have an addition height up to 350nm. The grains are not visible thanks to the rough top layer.

The last molecule under investigation, PTCDI-Ph, has a more smooth layer structure (rms

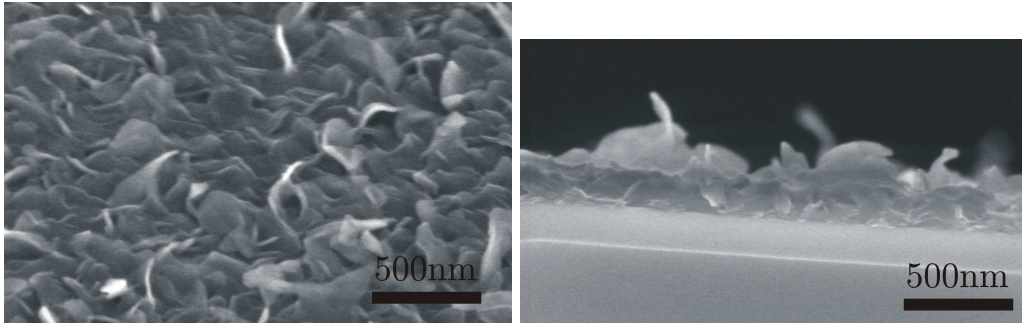


Figure 10: SEM picture of PTCDI-C13, top view (left) and cross-section view (right)

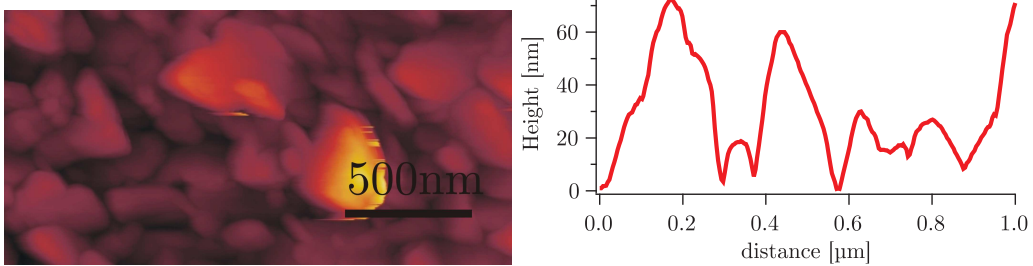


Figure 11: AFM picture of PTCDI-C13, top view (left) and a cross-section (right)

value of 11nm). Thickness determined by cross-section SEM is 160nm. The grains are small (200nm by 30nm) and hardly visible terraces have a height around 2nm.

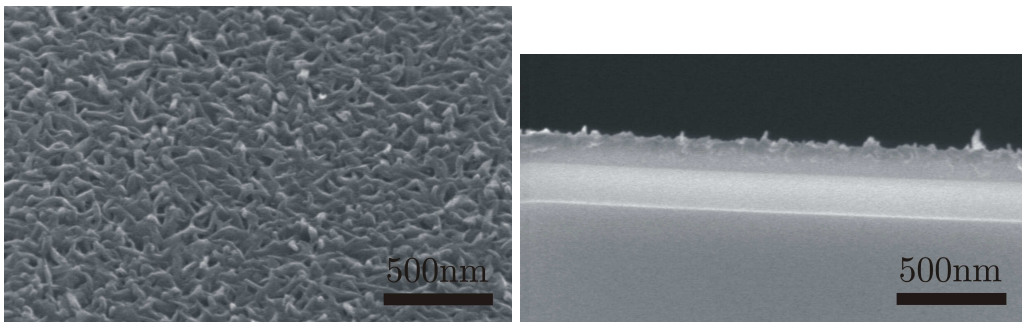


Figure 12: SEM picture of PTCDI-Ph, top view (left) and cross-section view (right)

### 3 Conclusions

To conclude, we investigated three perylene diimide derivatives, namely *N,N'*-Dialkyl-3,4,9,10-perylene tetracarboxylic diimides with alkyl=pentyl (PTCDI-C5), tridecyl (PTCDI-C13), and phenyl (PTCDI-Ph). Mobility measurements using photo-CELIV show a high mobility for PTCDI-C13 ( $10^{-4} \text{cm}^2/\text{Vs}$ ), a low mobility for PTCDI-C5 ( $10^{-6} \text{cm}^2/\text{Vs}$ ) with PTCDI-Ph in between ( $10^{-5} \text{cm}^2/\text{Vs}$ ). This corresponds to transistor measurements done in literature[2]. The explanation is the higher self-organisation of the molecules due to the increasing side-chain. This leads to higher intermolecular  $\pi$ -orbital overlap and a better conduction.

Absorbance measurement and ellipsometry show a lower absorption for the PTCDI-C13 compared to PTCDI-C5 and PTCDI-Ph. Again, the sidechains make the difference. As the interspac-

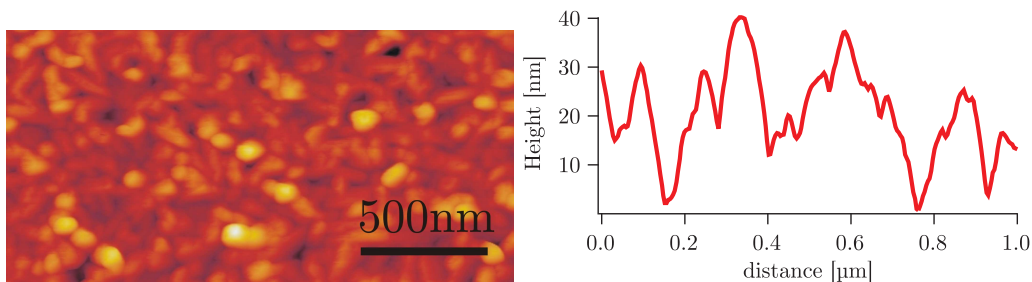


Figure 13: AFM picture of PTCDI-Ph, top view (left) and a crosssection (right)

ing in between two molecular layers increases due to the longer sidechain, the amount of molecules per unit volume will decrease. Assuming an equal absorption probability for each molecule, a denser film leads to a higher absorption coefficient.

In a last step, the morphology is investigated. The efficient self-organization of PTCDI-C13 leads to a rough layer while the two other layers have more smooth layers. A smooth layer is preferred when making diodes, as contacting rough layers is difficult.

## 4 Future collaborations

Possible future collaborations involve the fundamental optical and electrical study of different organic materials, both polymers and small molecules. As the two institutes have a complementary set of characterisation tools, a fast and efficient scan of new materials can be obtained. More exchange visits of people are planned in the near future.

## 5 Projected publications

As these results are an intermediate step to study organic solar cells based on perylene derivatives, more work has to be carried out before publications. Solar cells based on the different materials should be made and characterised.

## References

- [1] G. Horowitz, Kouki, Spearman, Fichou, Nogues, Pan, and Garnier. Evidence of n-type conduction in a perylene tetracarboxylic diimide derivative. *Adv. Mater.*, 8(3):242–245, 1996.
- [2] R. J. Chesterfield, J. C. McKeen, C. R. Newman, P. C. Ewbank, D. A. da Silva, J. L. Bredas, L. L. Miller, K. R. Mann, and C. D. Frisbie. Organic thin film transistors based on n-alkyl perylene diimides: Charge transport kinetics as a function of gate voltage and temperature. *J. Phys. Chem. B*, 108(50):19281–19292, December 2004.
- [3] Shuhei Tatemichi, Musubu Ichikawa, Toshiki Koyama, and Yoshio Taniguchi. High mobility n-type thin-film transistors based on N,N'-ditridecyl perylene diimide with thermal treatments. *Appl. Phys. Lett.*, 89(11):112108, 2006.
- [4] Soeren Steudel, Stijn de Vusser, Stijn de Jonge, Dimitri Janssen, Stijn Verlaak, Jan Genoe, and Paul Heremans. Influence of the dielectric roughness on the performance of pentacene transistors. *Appl. Phys. Lett.*, 85(19):4400–4402, 2004.
- [5] L. L. Chua, J. Zaumseil, J. F. Chang, E. C. W. Ou, P. K. H. Ho, H. Sirringhaus, and R. H. Friend. General observation of n-type field-effect behaviour in organic semiconductors. *Nature*, 434:194–198, March 2005.



- [6] M. Pope and C. E. Swenberg. *Electronic processes in organic crystals and polymers*. Oxford science publications, New York, 1999.
- [7] G. Juska, K. Arlauskas, M. Viliunas, and J. Kocka. Extraction current transients: new method of study of charge transport in microcrystalline silicon. *Phys. Rev. Lett.*, 84(21):4946–4949, 2000.
- [8] G. Juska, K. Arlauskas, M. Viliunas, K. Genevicius, R. Osterbacka, and H. Stubb. Charge transport in pi -conjugated polymers from extraction current transients. *Phys. Rev. B*, 62(24):R16235–R16238, 2000.
- [9] G. Juska, N. Nekrasas, K. Genevicius, J. Stuchlik, and J. Kocka. Relaxation of photoexcited charge carrier concentration and mobility in mu c-si:h. *Thin Solid Films*, 451-452:290–293, 2004.
- [10] A. J. Mozer, N. S. Sariciftci, L. Lutsen, D. Vanderzande, R. Osterbacka, M. Westerling, and G. Juska. Charge transport and recombination in bulk heterojunction solar cells studied by the photoinduced charge extraction in linearly increasing voltage technique. *Appl. Phys. Lett.*, 86(11):112104, 2005.
- [11] H. Bassler. Charge transport in disordered organic photoconductors - a monte-carlo simulation study. *Phys. Stat. Sol. B*, 175(1):15–56, 1993.